



Contents lists available at ScienceDirect

Journal of Biomechanics

journal homepage: www.elsevier.com/locate/jbiomech
www.JBiomech.com

Linear vs. non-linear mapping of peak power using surface EMG features during dynamic fatiguing contractions

M. Gonzalez-Izal^{a,b}, A. Malanda^a, I. Rodríguez-Carreño^c, I. Navarro-Amézqueta^b, E.M. Gorostiaga^b, D. Farina^d, D. Falla^d, M. Izquierdo^{b,*}

^a Department of Electric and Electronic Engineering, Public University of Navarre, Campus de Arrosadia, 31006 Pamplona, Spain

^b Studies, Research and Sport Medicine Center, Government of Navarre, C/Sanguesa 34, 31005 Pamplona, Spain

^c Department of Quantitative Methods, University of Navarre, Pamplona, Spain.

^d Center for Sensory-Motor Interaction, Department of Health Science and Technology, Aalborg University, Fredrik Bajers Vej 7, Bld. D3, DK-9220 Aalborg E, Denmark.

ARTICLE INFO

Article history:

Accepted 10 May 2010

Keywords:

Muscle fatigue
Neural network
Multivariable mapping
Electromyography
Dynamic contractions

ABSTRACT

This study compares a non-linear (neural network) and a linear (linear regression) power mapping using a set of features of the surface electromyogram recorded from the vastus medialis and lateralis muscles. Fifteen healthy participants performed 5 sets of 10 repetitions leg press using the individual maximum load corresponding what they could perform 10 times (10RM) with 120 s of rest between them. The following sEMG variables were computed from each extension contraction and used as inputs to both approaches: mean average value (MAV), median frequency (Fmed), the spectral parameter proposed by Dimitrov (Flnsm5), average (over the observation interval) of the instantaneous mean frequency obtained from a Choi-Williams distribution (MFM), and wavelet indices ratio between moments at different scales (WIRM1551, WIRM1M51, WIRM1522, WIRE51, and WIRW51). The non-linear mapping (neural network) provided higher correlation coefficients and signal-to-noise ratios values (although not significantly different) between the actual and the estimated changes of power compared to linear mapping (linear regression) using the sEMG variables alone and a combination of WIRW51 and MFM (obtained by a stepwise multiple linear regression). In conclusion, non-linear mapping of force loss during dynamic knee extension exercise showed higher signal-to-noise ratio and correlation coefficients between the actual and estimated power output compared to linear mapping. However, since no significant differences were observed between linear and non-linear approaches, both were equally valid to estimate changes in peak power during fatiguing repetitive leg extension exercise.

© 2010 Published by Elsevier Ltd.

1. Introduction

Manifestations of muscle fatigue can be defined on the basis of electrophysiological or mechanical events. In this work, muscle fatigue is defined as a failure to maintain the required or expected force (Edwards, 1981). Changes in mechanical power output during fatiguing activities can be due to many peripheral factors such as accumulation of lactate, H⁺ inorganic phosphate (Pi) and ammonia, decreased number and force of cross bridges, decreased myofibrillar Ca²⁺ sensitivity, and a decline in muscle adenine nucleotide stores, mainly through a pronounced reduction in muscle ATP content (Fitts, 1994; Hellsten et al., 1996; Karlsson and Saltin, 1971; Mohr et al., 2007; Sahlin and Henriksson, 1984). Both amplitude and spectral features of the surface electromyography (sEMG) signals are known to be influenced by muscle

fatigue. Changes in sEMG amplitude during fatiguing contractions are related to recruitment of additional active motor units (Moritani et al., 1982), rise in MU firing frequency (Bigland-Ritchie et al., 1983) as well as to peripheral factors inducing changes in amplitudes of motor unit potentials (i.e. lengthening of intracellular action potential) (Arabadzhev et al., 2010). Changes in spectral features are related to changes in the duration of the motor unit action potential waveform and the subsequent changes in muscle fiber conduction velocities (Bigland-Ritchie et al., 1981). Thus, monitoring the associations between sEMG variables and muscle fatigue has been traditionally performed to estimate muscle fatigue.

Several attempts have been made to develop models that associate changes in sEMG variables to power/torque loss (as a direct measurement of muscle fatigue) during maximal dynamic contractions. Linear models based on linear regression have shown that the median frequency provides a better estimation of torque loss than the amplitude of the sEMG signal during maximal isokinetic exercises since the correlation coefficient with

* Corresponding author. Tel.: +34 948 292623; fax: +34 948 292636.
E-mail address: mikel.izquierdo@gmail.com (M. Izquierdo).

torque loss were higher (Gerdle et al., 2000). Moreover, the spectral parameter proposed by Dimitrov (2006) accounted for 37% of the performance variance of changes in peak power during dynamic leg extension exercises. In addition, when this parameter is combined with the average (over the observation interval) instantaneous mean frequency as a two factor combination predictor, it accounts for 44% of changes in power (Gonzalez-Izal et al., 2010). However, associations between sEMG variables and muscle fatigue are likely to be non-linear. Therefore, non-linear models have also been developed based on the learning procedure of a neural network capable of identifying these non-linear relations. Maclsaac et al. (2006) used a neural network to combine different time and spectral features of the sEMG signal into a fatigue index which was reported to show better accuracy to track myoelectric manifestations of fatigue than mean frequency or instantaneous mean frequency alone. However, both approaches (linear and non-linear) have not been directly compared to determine which is superior to identify the associations between muscle fatigue and sEMG-based parameters.

We hypothesized that due to the complex relation between features of the sEMG signals and muscle fatigue, a non-linear model based on a learning procedure would provide a more accurate tracking of power loss using sEMG variables compared to a linear model. Thus, the aim of this study was to compare the accuracy of a fatigue linear model (linear regression) and a non-linear model (based on a neural network) to relate sEMG variables to power loss during repetitive maximal leg extensions.

2. Material and methods

2.1. Subjects

Fifteen healthy and physically active men (age, mean \pm SD, 34.2 ± 5.2 yr; height, 177.3 ± 5.6 cm; body mass, 73.1 ± 6.4 kg) volunteered to participate in the study. Subjects provided informed written consent. The study was conducted in accordance with the Declaration of Helsinki and approved by the Institutional Review Committee of the Instituto Navarro del Deporte.

2.2. Experimental procedure

The protocol consisted of 5 sets of 10 repetitions of maximum leg presses using the individual maximum load corresponding what they could perform 10 times (10RM) with 120 s of rest between sets (Gonzalez-Izal et al., 2010). Each trial (i.e. leg press action in a sitting position) was performed on a bilateral leg extension exercise machine (Technogym, Gambettola, Italy). The trial began with a knee angle of 90° and a hip angle of 45° , and ended when subjects extended their legs (knee angle of 180° and a hip angle of 90°). The seat was individually adjusted to minimize displacement between the lower back and the backrest during muscular force exertion. Strong verbal encouragement was given to all the subjects to motivate them to perform each test action as maximally and as rapidly as possible. The subjects were asked to eat similar diets before the loading sessions. Subjects did not perform any strenuous exercise for 48 h before the experimental exercise session

2.3. Data acquisition

Peak power of the leg extension obtained as the maximum value of the product between the exerted force and the velocity of movement and sEMG of the vastus medialis (VM) and lateralis (VL) were concurrently measured during the exercise. The peak power was calculated from the power signal during the extension exercise. The sEMG signals were recorded with pairs of bipolar surface electrodes placed longitudinally on the middle portion of the muscle (Blue Sensor N-00-S, Medicotest) with an interelectrode distance of 22 mm, following the recommendations of the SENIAM (Surface ElectroMyoGraphy for the Non-Invasive Assessment of Muscles).

EMG signals were recorded at a sampling rate of 1 kHz with a Muscle Tester ME3000 (Mega Electronics Ltd.) (bandwidth of 8–500 Hz/3 dB and a common mode rejection ratio > 100 dB). To facilitate and normalize the analysis, the knee movement was divided into 4 intervals of 22.5° . The parameters analyzed in the present study corresponded to the first interval of the movement of the dynamic contractions (from 90° to 112.5° of knee movement).

2.4. Signal analysis

Signal analysis was performed off-line using Matlab 2008b (The MathWorks Inc., Natick, Massachusetts, USA). The following sEMG variables were computed from each extension contraction: mean average value (MAV), median frequency (Fmed), the spectral parameter proposed by Dimitrov et al. (2006) (Flnsm5), the average (over the observation interval) of the instantaneous mean frequency obtained from a Choi–Williams distribution (Choi and Williams, 1989) (MFM), and wavelet index ratios between moments at different scales.

- 1) MAV was calculated as the integrated EMG divided by the integration time.
- 2) Fmed was estimated from the power spectrum calculated using Fast Fourier Transform.
- 3) The spectral parameter proposed by Dimitrov et al. (2006) (Flnsm5) is as follows:

$$\text{Flnsm5} = \frac{\int_{f_1}^{f_2} f^{-1} \text{PS}(f) df}{\int_{f_1}^{f_2} f^5 \text{PS}(f) df} \quad (1)$$

where $\text{PS}(f)$ is the EMG power spectrum calculated using Fast Fourier Transform, $f_1=8$ Hz and $f_2=500$ Hz (determined from the bandwidth of the EMG amplifier).

This parameter was designed to overcome the low sensitivity to muscle fatigue of the median frequency. It relates the spectral moment of order (-1) and the spectral moment of order 5. The spectral moment of order (-1) emphasizes the increase in low frequencies of the EMG spectrum related to increased negative afterpotentials during muscular fatigue. The spectral moment of order 5 emphasizes the decreases in the high frequencies related to increments in the duration of the intracellular action potentials and decrements in the velocity of the action potential propagation velocity.

- 4) Average (over the observation interval) of the instantaneous mean frequency (IMF) obtained from a Choi and Williams (1989) (MFM):

$$\text{IMF}(t) = \frac{\int_{f_1}^{f_2} f \text{PS}_{\text{cw}}(f,t) df}{\int_{f_1}^{f_2} \text{PS}_{\text{cw}}(f,t) df} \quad (2)$$

where $\text{PS}_{\text{cw}}(f,t)$ is the time-dependent power spectrum obtained from the Choi–Williams distribution and again, $f_1=8$ Hz and $f_2=500$ Hz.

- 5) Wavelet indices ratios between moments at different scales. The discrete wavelet transform (DWT) is a technique that simultaneously obtains a time and a scale representation of signals. Its implementation can be performed by repeatedly filtering the signal with a pair of filters. Specifically, the DWT decomposes a signal into an approximation signal using a low-pass filter $h[n]$ and a detail signal using a high-pass filter $g[n]$. Both low-pass and high-pass filters are synthesized from the wavelet function $\psi(t)$ and from the scaling function $\phi(t)$, respectively. The approximation signal is subsequently divided into new approximation and detail signals. This process is carried out iteratively producing a set of approximation signals at different detail levels (scales) and a final gross approximation of the signal. The detail D_j and the approximation A_j at level j can be obtained by filtering the signal with h and g , respectively. A different formulation of the DWT based on a filter bank can also be found (Strang and Nguyen, 1996).

The DWT was calculated using Mallat's (1992) algorithm. We used the interpolated versions of the detail and approximation signals, without downsampling (stationary wavelet transform, SWT), so that we ended up with the same number of time samples in each of the calculated signals (detail and approximation signals). We tried different wavelet functions $\psi(t)$ to calculate the wavelet indices and finally we chose the Symlet 5 (sym5) (Daubechies, 1992) and the Daubechies 5 (db5) (Daubechies, 1988), where 5 is the number of vanishing moments of both symlet and Daubechies mother wavelet. The higher the degrees of vanishing moments a wavelet has, the better it models the smooth part of a signal. Both wavelets have previously been applied for feature extraction from sEMG signals with successful results (Englehart et al., 1999; Rodriguez and Vuskovic, 2007).

Fig. 1 shows the frequency bands related to some detail signals from the SWT calculated using sym5. It can be appreciated that they correspond to a filter bank with constant Q . Besides, Table 1 shows the maximum frequency (F_{max}) (frequency of the peak amplitude of the spectrum) and the range of frequencies corresponding to these wavelet scales.

Four parameters were calculated from spectral moments:

- 5.1) Wavelet ratio between moment -1 at scale 5 and moment 5 at scale 1 (WIRM1551):

$$\text{WIRM1551} = \frac{\int_{f_1}^{f_2} f^{-1} D_5(f) df}{\int_{f_1}^{f_2} f^5 D_1(f) df} \quad (3)$$

where $D_5(f)$ and $D_1(f)$ are the power spectra of the fifth and first scales, respectively, of the SWT using the sym5 wavelet, and $f_1=8$ Hz and $f_2=500$ Hz.

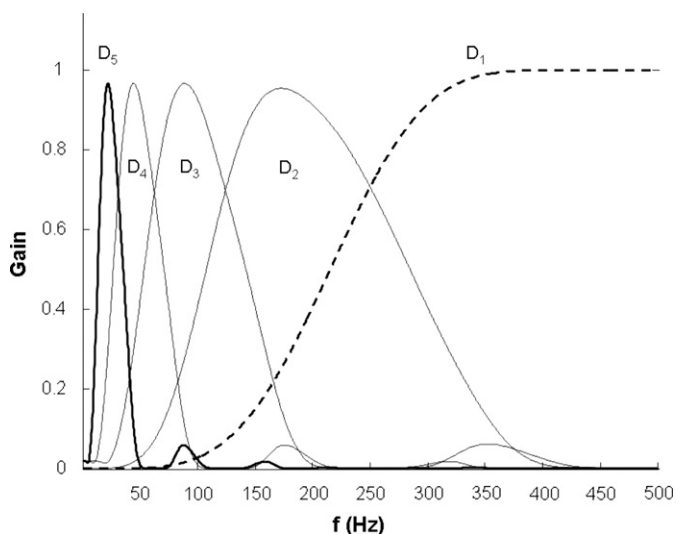


Fig. 1. Frequency bands (calculated using the discrete Fourier Transform) of the first five DWT details obtained using wavelet sym5. D_5 (thick line) and D_1 (thick dashed line) are the wavelet scales used to calculate WIRM1551, WIRM1M51, WIRE51, and WIRW51.

Table 1

Correlation coefficient (R) and signal-to-noise ratio (SNR) between changes in peak power output and estimated changes in peak power output using a non-linear mapping (multi-layer perceptron neural network) and linear mapping (linear regression). The force loss prediction was estimated for both approaches using the sEMG-based parameters individually as inputs.

	Linear mapping (linear regression) R (SNR)	Non-linear mapping (MLP neural network) R (SNR)
MAV	-0.34 (5.66)	-0.38 (5.73)
Fmed	0.49 (6.12)	0.52 (6.23)
log Flnsm5	-0.59 (6.60)	-0.68 (7.22)
MFM	0.57 (6.47)	0.62 (6.79)
log WIRM1551	-0.70 (7.45)	-0.74 (7.96)
log WIRM1M51	-0.70 (7.46)	-0.75 (8.00)
log WIRW51	-0.72 (7.61)	-0.76 (8.12)
log WIRE	-0.71 (7.54)	-0.75 (8.09)
log WIRM1522	-0.71 (7.50)	-0.75 (7.99)

5.2) Wavelet ratio between moment -1 at maximum energy scale and moment 5 at scale 1 (WIRM1M51):

$$\text{WIRM1M51} = \frac{\int_{f_1}^{f_2} f^{-1} D_{\max}(f) df}{\int_{f_1}^{f_2} f^5 D_1(f) df} \quad (4)$$

where $D_{\max}(f)$ and $D_1(f)$ are the power spectra of the maximum energy scale and the first scale, respectively, of the SWT using the db5 wavelet, and $f_1 = 8$ Hz and $f_2 = 500$ Hz. The maximum energy scale in this work was usually scale 4.

5.3) Wavelet ratio between moment -1 at scale 5 and moment 2 at scale 2 (WIRM1522):

$$\text{WIRM1522} = \frac{\int_{f_1}^{f_2} f^{-1} D_5(f) df}{\int_{f_1}^{f_2} f^2 D_2(f) df} \quad (5)$$

where $D_5(f)$ and $D_2(f)$ are the power spectra of the fifth and second scales, respectively, of the SWT using the db5 wavelet, and $f_1 = 8$ Hz and $f_2 = 500$ Hz.

5.4) Wavelet ratio of energies at scales 5 and 1 (WIRE51):

$$\text{WIRE51} = \frac{\sum_{i=1}^N D_5^2[n]}{\sum_{i=1}^N D_1^2[n]} \quad (6)$$

where $D_5[n]$ and $D_1[n]$ are the detail signals at scales five and one, respectively, of the SWT calculated using the sym5 wavelet.

5.5) Wavelet ratio between square waveform lengths at different scales (WIRW51).

The waveform length is a parameter that measures the cumulative changes in amplitude from time sample to time sample over the whole

signal. The waveform length effectively encapsulates the amplitude, frequency, and duration of the EMG signal in one simple formula (Zecca et al., 2002). The index was calculated as

$$\text{WIRW51} = \frac{\sum_{i=2}^N |D_5[i] - D_5[i-1]|^2}{\sum_{i=2}^N |D_1[i] - D_1[i-1]|^2} \quad (7)$$

where $D_5[n]$ and $D_1[n]$ are the details at scales five and one, respectively, of the SWT calculated using the sym5 wavelet.

An average of the sEMG parameters obtained from the VM and VL was calculated as a more representative index of muscle extension.

2.5. Multi-layer perceptron neural network

An artificial neural network is a mathematical model formed by an interconnected group of artificial neurons and its structure changes depending on the information received during the learning phase. The artificial neural network chosen to relate changes in sEMG variables and power in the present study was the multi-layer perceptron (MLP), which shows good accuracy to relate sEMG variables and fatigue indices (MacIsaac et al., 2006). The MLP consists of a combination of different layers of perceptrons which combines its inputs after weighting them with an appropriate weight. The training phase (also called learning phase) of the MLP consists of changing these weights to minimize the errors between the desired and the corresponding outputs. The training and testing of the MLP were performed using Matlab Neural Network Toolbox (The MathWorks Inc, Natick, Massachusetts, USA).

2.6. Force loss prediction

Non-linear mapping and linear regressions were used to relate sEMG variables of all the subjects to peak power output. The power loss was estimated using the sEMG variables individually and in combination.

The performance of the approaches was quantified by the signal-to-noise ratio (SNR) for the outputs:

$$\text{SNR} = \frac{R}{\sqrt{\frac{1}{N} \sum_{n=1}^N (I_n - \hat{I}_n)^2}} \quad (8)$$

where R represents the range of the desired outputs (calculated as the maximum minus the minimum of the percentage change in power) and the denominator represents the root mean square error between the estimated (\hat{I}_n) and desired outputs (I_n), across N contractions.

2.7. Statistical analysis

Changes in percentage between each variable (i.e. sEMG-based parameters and peak power output) and the average of the values of the first two contractions were calculated. The percentage changes that did not follow a normal distribution were log-transformed (Flnsm5 and wavelet-based parameters).

Pearson product-movement correlation coefficients (R) were used to determine the association between changes in real and estimated values of peak power output. A stepwise multiple linear regression analysis was used to combine two or more sEMG-based parameters with power output changes.

To test the similarity of slopes and intercepts of the relationships between actual and estimated changes in peak power outputs obtained from both approaches (using a MLP and linear regressions), the corresponding t -test was applied for the model: $Y_{ij} = \alpha_i + \beta_i X_{ij} + \varepsilon_{ij}$ for $i = 1, 2$ ($1 = \text{MLP}$; $2 = \text{linear regression}$) and $j = 1, \dots, n_1$ being ε_{ij} i.i.d. random variables following a distribution $N(0, \sigma_1)$. Statistical significance was set at $P < 0.05$.

3. Results

Peak power output of the last five repetitions of each set was significantly lower ($P < 0.05$) than that attained during the first five repetitions of the exercise. Moreover, the peak power output attained during the last repetition of the fifth set was 45% lower than that attained during the initial two repetitions of the first set.

Fig. 2 illustrates the evolution of muscle power output and the sEMG signals and its power spectrum recorded from the vastus medialis during the 2nd contraction of the 1st set (one at the beginning of the protocol) and during the last contraction of the 4th set (at the final of the protocol). As the figure showed, the contraction at the final of the protocol was longer and the peak power was lower (Fig. 2b) than the one at the beginning of the

protocol (Fig. 2a). Moreover, the power spectrum attained to the final of the protocol (Fig. 2f), had shifted to lower frequencies compared to the one at the beginning of the protocol (Fig. 2e).

Fig. 3 illustrates the actual vs. the estimated changes in power output obtained for both approaches (linear and non-linear models) using some sEMG-based parameters of all the subjects as input variables. The non-linear mapping (MLP) showed higher signal-to-noise ratio and correlation coefficients between the actual and estimated power output compared to that obtained using linear mapping (Table 1). However, no significant differences were observed for the slopes and intercepts of the

regression lines between the actual and estimated power output obtained using both approaches.

The stepwise multiple linear regression showed that the combination of log WIRW51 and MFM provided more accurate power mapping in a linear mapping than other combinations of two sEMG-based parameters. Moreover, after combining all the sEMG variables in groups of two using a neural network (non-linear mapping) and comparing its performance to map changes in peak power, the same combination of log WIRW51 and MFM provided more accurate power mapping. Using this combination of sEMG-based parameters the neural network also provided a

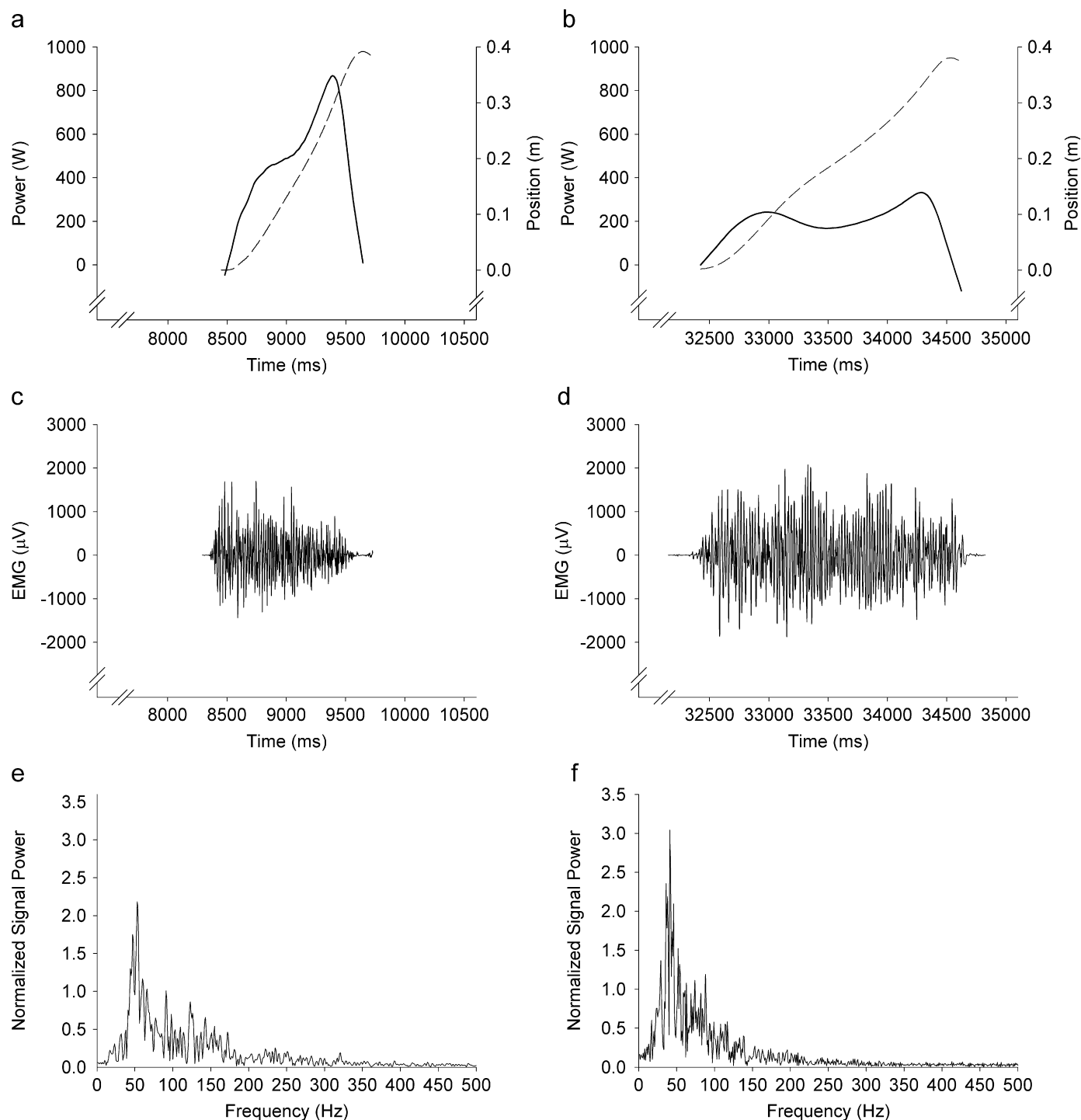


Fig. 2. Power (solid line) and position of the load (dashed line), (a, b) EMG of the vastus medialis (c, d) and its power spectrum (e, f) during the second contraction of the 1st set (in the left) and during the last contraction of the 4th set (in the right).

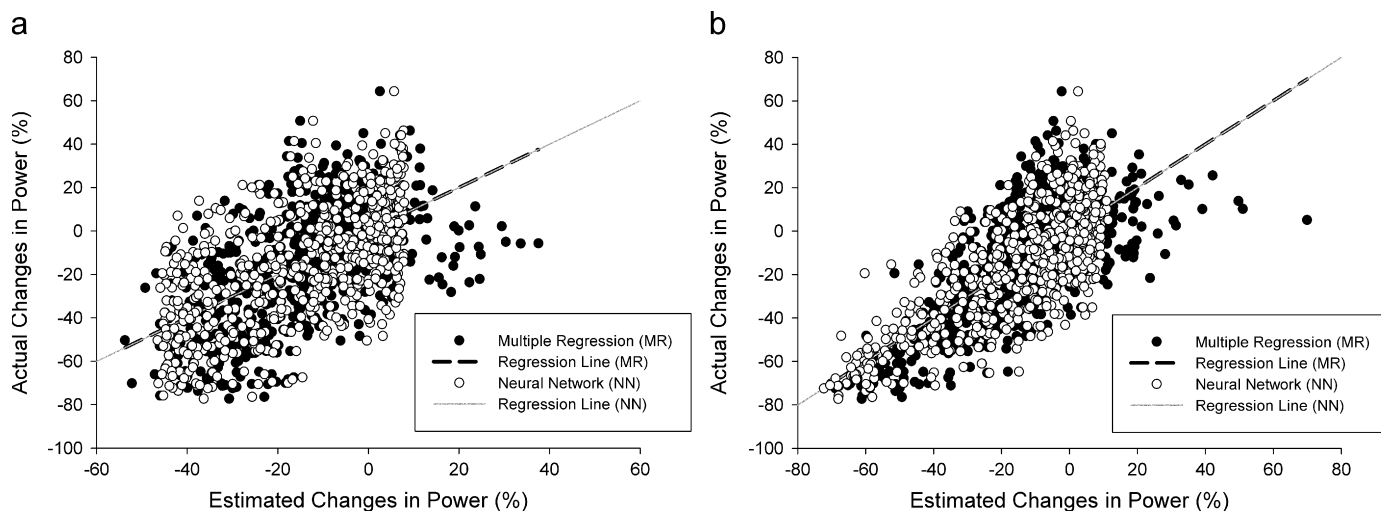


Fig. 3. Actual vs. estimated changes in power output obtained for both approaches (linear and non-linear models) using sEMG-based parameters of all the subjects as input variables: (a) average (over the observation interval) of the instantaneous mean frequency and (b) log WIRW51.

higher signal-to-noise ratio and a higher correlation coefficient ($R=0.77$; $SNR=8.42$) compared to multiple linear regression ($R=0.73$; $SNR=7.77$). However, the comparison between the regression lines of the actual vs. the estimated changes in power output for both approaches did not reach statistical significance.

4. Discussion

This study showed that the correlation coefficients obtained between the actual and the estimated changes of power output using the non-linear mapping (neural network) were higher compared to those obtained using linear mapping (linear regression). Moreover, the signal-to-noise ratios were also higher and, therefore, the estimation errors were smaller using a non-linear mapping approach. However, no significant differences were observed in the slope and intercepts of the regression lines calculated from the data (actual power output vs. estimated power output) obtained for both approaches. Thus, both linear and non-linear mappings were equally capable of estimating changes in power output from sEMG features during repetitive dynamic leg extensions. In contrast with the present results, during isometric, isokinetic, and random elbow flexions and extensions, the accuracy of myoelectric manifestations of fatigue were better tracked with a non-linear multivariable myoelectric mapping function compared to the mean frequency or instantaneous mean frequency alone (Maclsaac et al., 2006). However, in the present study power loss was tracked whereas Maclsaac et al. (2006) tracked myoelectric changes over time. Moreover, different muscle groups were involved and different types of muscle actions were performed. It is unknown whether non-linear and linear mapping would be equally valid to track power loss from myoelectric variables during other contraction types (i.e. isometric or submaximal fatiguing exercises). During these conditions the relationship between sEMG-based parameters and power loss may not be linear and therefore a non-linear approach may be more appropriate. Moreover, a non-linear approach may be more accurate if a single model is required to map force loss during isometric, submaximal, and maximal fatiguing exercises at different velocities of execution. Besides, in other kinds of analysis as movement pattern recognition the non-linear approaches probably provide better results than linear models (Kelly et al., 1990).

In summary, non-linear mapping of force loss during dynamic knee extension exercise showed higher signal-to-noise ratio and

correlation coefficients between the actual and estimated power output compared to linear mapping. However, since no significant differences were observed between linear and non-linear approaches, both were equally valid to estimate changes in peak power during fatiguing repetitive leg extension exercise. Nevertheless, as linear mapping implies less computational time than non-linear mapping (training the neural network), it is preferable to map changes in peak power using sEMG variables.

Conflict of interest statement

None of the authors have a conflict of interest.

Acknowledgments

This study was partly supported by a grant of the University Public of Navarre, the Spanish Ministry of Education (National Plan of R&D+I 2004–2007. Key Action “Sport and Physical Activity” DEP2006–56076).

References

- Arabadzhev, T.I., Dimitrov, V.G., Dimitrova, N.A., Dimitrov, G.V., 2010. Interpretation of EMG integral or RMS and estimates of “neuromuscular efficiency” can be misleading in fatiguing contraction. *Journal of Electromyography and Kinesiology* 20, 223–232.
- Bigland-Ritchie, B., Donovan, E.F., Roussos, C.S., 1981. Conduction velocity and EMG power spectrum changes in fatigue of sustained maximal efforts. *Journal of Applied Physiology* 51, 1300–1305.
- Bigland-Ritchie, B., Johansson, R., Lippold, O.C., Smith, S., Woods, J.J., 1983. Changes in motoneurone firing rates during sustained maximal voluntary contractions. *Journal of Physiology* 340, 335–346.
- Choi, H.I., Williams, W.J., 1989. Improved time–frequency representation of multicomponent signals using exponential kernels. *IEEE Transactions on Acoustics, Speech and Signal Processing* 37, 862–871.
- Daubechies, I., 1988. Orthonormal bases of compactly supported wavelets. *Communications on Pure and Applied Mathematics* 41, 909–996.
- Daubechies, I., 1992. Ten lectures on wavelets. CBMS-NSF Regional Conference Series in Applied Mathematics, vol. 61. SIAM, Philadelphia.
- Dimitrov, G.V., Arabadzhev, T.I., Mileva, K.N., Bowtell, J.L., Crichton, N., Dimitrova, N.A., 2006. Muscle fatigue during dynamic contractions assessed by new spectral indices. *Medicine and Science in Sports and Exercise* 38, 1971–1979.
- Edwards, R.H., 1981. Human muscle function and fatigue. *Ciba Foundation Symposium* 82, 1–18.
- Englehart, K., Hudgins, B., Parker, P.A., Stevenson, M., 1999. Classification of the myoelectric signal using time–frequency based representations. *Medical Engineering and Physics* 21, 431–438.

- Fitts, R.H., 1994. Cellular mechanisms of muscle fatigue. *Physiological Reviews* 74, 49–94.
- Gerdle, B., Larsson, B., Karlsson, S., 2000. Criterion validation of surface EMG variables as fatigue indicators using peak torque: a study of repetitive maximum isokinetic knee extensions. *Journal of Electromyography and Kinesiology* 10, 225–232.
- Gonzalez-Izal, M., Malanda, A., Navarro-Amezqueta, I., Gorostiaga, E.M., Mallor, F., Ibanez, J., Izquierdo, M., 2010. EMG spectral indices and muscle power fatigue during dynamic contractions. *Journal of Electromyography and Kinesiology* 20, 233–240.
- Hellsten, Y., Apple, F.S., Sjodin, B., 1996. Effect of sprint cycle training on activities of antioxidant enzymes in human skeletal muscle. *Journal of Applied Physiology* 81, 1484–1487.
- Karlsson, J., Saltin, B., 1971. Oxygen deficit and muscle metabolites in intermittent exercise. *Acta Physiologica Scandinavica* 82, 115–122.
- Kelly, M.F., Parker, P.A., Scott, R.N., 1990. The application of neural networks to myoelectric signal analysis: a preliminary study. *IEEE Transactions on Biomedical Engineering* 37, 221–230.
- MacIsaac, D.T., Parker, P.A., Englehart, K.B., Rogers, D.R., 2006. Fatigue estimation with a multivariable myoelectric mapping function. *IEEE Transactions on Biomedical Engineering* 53, 694–700.
- Mallat, S., 1992. Characterization of signals from multiscale edges. *IEEE Transactions on Pattern Analysis Machine Intelligence* 14, 710–732.
- Mohr, M., Krstrup, P., Nielsen, J.J., Nybo, L., Rasmussen, M.K., Juel, C., Bangsbo, J., 2007. Effect of two different intense training regimens on skeletal muscle ion transport proteins and fatigue development. *American Journal of Physiology—Regulatory, Integrative and Comparative Physiology* 292, 1594–1602.
- Moritani, T., Nagata, A., Muro, M., 1982. Electromyographic manifestations of muscular fatigue. *Medicine and Science in Sports and Exercise* 14, 198–202.
- Rodriguez, I., Vuskovic, M., 2007. Wavelet transform moments for feature extraction from temporal signals, *Informatics in Control, Automation and Robotics II*. Springer, Netherlands, pp. 235–242.
- Sahlin, K., Henriksson, J., 1984. Buffer capacity and lactate accumulation in skeletal muscle of trained and untrained men. *Acta Physiologica Scandinavica* 122, 331–339.
- Strang, G., Nguyen, T., 1996. *Wavelets and Filter Banks*. Wellesley-Cambridge Press.
- Zecca, M., Micera, S., Carrozza, M.C., Dario, P., 2002. Control of multifunctional prosthetic hands by processing the electromyographic signal. *Critical Reviews in Biomedical Engineering* 30, 459–485.